Acta Crystallographica Section D
Biological Crystallography
ISSN 0907-4449

Beyond the detergent effect: a binding site for sodium dodecyl sulfate (SDS) in mammalian apoferritin

Renyu Liu,[a]* Weiming Bu,[a] Jin Xi,[a] Shirin R. Mortazavi,[b] Jasmina C. Cheung-Lau,[a] Ivan J. Dmochowski[c] and Patrick J. Loll[b]*

[a]Department of Anesthesia and Critical Care, University of Pennsylvania, Philadelphia, Pennsylvania, USA, [b]Department of Biochemistry and Molecular Biology, Drexel University College of Medicine, Philadelphia, Pennsylvania, USA, and [c]Department of Chemistry, University of Pennsylvania, Philadelphia, Pennsylvania, USA

Correspondence e-mail: renyu.liu@uphs.upenn.edu, ploll@drexelmed.edu

Received 28 October 2011
Accepted 21 January 2012

PDB Reference: SDS–apoferritin complex, 3u90.

Although sodium dodecyl sulfate (SDS) is widely used as an anionic detergent, it can also exert specific pharmacological effects that are independent of the surfactant properties of the molecule. However, structural details of how proteins recognize SDS are scarce. Here, it is demonstrated that SDS binds specifically to a naturally occurring four-helix bundle protein: horse apoferritin. The X-ray crystal structure of the apoferritin–SDS complex was determined at a resolution of 1.9 Å and revealed that the SDS binds in an internal cavity that has previously been shown to recognize various general anesthetics. A dissociation constant of 24 ± 9 μM at 293 K was determined by isothermal titration calorimetry. SDS binds in this cavity by bending its alkyl tail into a horseshoe shape; the charged SDS head group lies in the opening of the cavity at the protein surface. This crystal structure provides insights into the protein–SDS interactions that give rise to binding and may prove useful in the design of novel SDS-like ligands for some proteins.

1. Introduction

Sodium dodecyl sulfate (SDS) is an anionic detergent with a 12-carbon tail attached to a sulfate group and is a familiar and widely used surfactant in biochemical experiments. Less well appreciated is the fact that SDS can also exert specific pharmacological effects that are unrelated to its surfactant behavior. For example, SDS is an antagonist for the human neutrophil formyl-peptide receptor (Thorén *et al.*, 2010) and it can activate the superoxide-generating NADPH-oxidase complex in cell-free systems (Clark *et al.*, 1987). Such receptor-mediated effects imply specific recognition of the ligand by one or more proteins. However, the structural details of how SDS is recognized by proteins are not fully appreciated. In this communication, we report that SDS binds to apoferritin and use this protein to investigate the molecular details of SDS recognition.

Apoferritin is a predominantly intracellular protein with iron-uptake and mineralization activity. 24 individual four-helix-bundle protomers associate to form a hollow structure with octahedral symmetry (for a recent review of ferritin structure, see Crichton & Declercq, 2010). We have previously discovered that apoferritin binds general anesthetics with affinities that are comparable to their clinical potencies (Liu *et al.*, 2005; Vedula *et al.*, 2009). To our knowledge, anesthetic binding by apoferritin plays no clinically significant role in

anesthesia; however, because apoferritin is stable and can easily be crystallized, it is a highly tractable model system for structural studies of protein–anesthetic interactions. The anesthetic binding site has been mapped by crystallographic analysis of multiple apoferritin–anesthetic complexes and has been found to localize to a cavity lying at the interface between two apoferritin protomers (Vedula *et al.*, 2009; Liu *et al.*, 2005). Affinities for this site were explored for a series of analogs of the general anesthetic propofol and were found to be strongly correlated with the ability of each analog to potentiate GABA responses at the GABA(A) receptor, implying that the structure of the apoferritin site may resemble that of an anesthetic binding site on the GABA(A) receptor (Vedula *et al.*, 2009). Interestingly, SDS has also been found to enhance GABA responses at the GABA(A) receptor (Yang & Sonner, 2008), suggesting that it might share the same or similar binding sites as anesthetics when binding to protein targets. In particular, it seemed likely that SDS could occupy the anesthetic binding site in apoferritin. In this study, we tested this hypothesis using solution calorimetry and high-resolution X-ray crystallography.

2. Materials and methods

2.1. Materials

Horse spleen apoferritin was purchased from Sigma Chemical Co. (St Louis, Missouri, USA) and was used without further purification. This preparation of horse spleen apoferritin contains two different polypeptide chains, namely the heavy (H) and light (L) chains, with the L chain making up 85–90% of the total protein. H and L chains are assumed to be randomly incorporated into the 24-mer (Harrison & Arosio, 1996). Other chemicals, including SDS, were also obtained from Sigma and were of reagent grade.

2.2. Isothermal titration calorimetry (ITC)

ITC measurements were carried out at 293 K using a VP-ITC instrument (MicroCal Inc., Northampton, Massachusetts, USA) essentially as described previously (Liu & Eckenhoff, 2005). The sample cell (1.43 ml) contained 0.01 m*M* apoferritin in 130 m*M* NaCl, 20 m*M* sodium phosphate pH 7.0 and the reference cell contained water. SDS (3.47 m*M*) was dissolved in the same buffer as the protein. The titration volumes were 1 µl for the first injection and 15 µl thereafter, with 5 min intervals between the injections. The data were corrected for heats of dilution using titrations of ligand into buffer, buffer into protein and buffer into buffer. Importantly, the titration of concentrated SDS solutions into buffer did not yield a significant heat signature, revealing that under these conditions the enthalpy of micelle dissipation is small relative to the heat of binding (Supplementary Fig. S1[1]). The enthalpy data were fitted to a model using a single set of independent sites using *Origin* 5.0 (Microcal Inc.) as described previously (Liu *et al.*, 2005; Liu & Eckenhoff, 2005). For the competition analysis, two separate types of experiments were performed. In the first series of experiments, 10 m*M* isoflurane was titrated into 0.01 m*M* apoferritin in the presence or absence of a saturating concentration of SDS. In the second series of experiments, 3.47 m*M* SDS was titrated into 0.01 m*M* apoferritin in the presence or absence of 10 m*M* isoflurane.

Table 1
Crystallographic data-collection and refinement statistics for apoferritin–SDS.

Values in parentheses are for the outermost resolution shell.

Data collection	
Space group	*F*432
Resolution range (Å)	19.84–1.90 (1.96–1.90)
Unit-cell parameters (Å)	$a = b = c = 181.83$
No. of unique reflections	25626
Mean multiplicity	34.09 (34.09)
Completeness	98.6 (87.9)
$R_{\rm merge}$	0.088 (0.387)
Mean $I/\sigma(I)$	43.4 (9.0)
Refinement	
$R_{\rm work}$	0.1847
$R_{\rm free}$	0.2074
No. of atoms	
Total	1552
Protein	1355
Ligand	17
Water	170
Metal	10
Mean *B* values (Å^2)	
Protein	21.8
Ligand	22.8
Water	29.0
Metals	46.3
R.m.s. deviations from ideality	
Bonds (Å)	0.006
Angles (°)	0.900
Ramachandran plot statistics, residues in	
Most favored regions (%)	98.8
Additionally allowed regions (%)	1.2

2.3. Circular-dichroism (CD) spectroscopy

Far-UV CD spectra were measured for apoferritin in the presence of SDS using a Chirascan CD Spectrometer (Applied Photophysics Limited, Leatherhead, England). Spectra were recorded at 298 K using rectangular cuvettes with path length 1 mm and were analyzed using the Applied Photophysics software package *CDNN*. The percentage of α-helical content was estimated by measuring the mean residue ellipticity at 222 nm. The protein concentration was 1 µ*M* in 10 m*M* sodium phosphate pH 7.0; spectra were measured in the presence and absence of 347 µ*M* SDS.

2.4. Protein crystallization and structure determination

Large single crystals were grown using hanging-drop vapor diffusion. The reservoir solution consisted of 0.05 *M* cadmium sulfate, 0.1 *M* HEPES and 1.0 *M* sodium acetate pH 7.5; the protein solution consisted of 12 mg ml^{-1} apoferritin in 0.03 *M* NaCl plus 1.7 m*M* SDS. The protein solution was mixed with reservoir buffer in a 1:1 ratio and the drop was incubated at 277 K; the crystals grew to full size in one week. Before data collection, the crystals were cryoprotected in reservoir buffer

[1] Supplementary material has been deposited in the IUCr electronic archive (Reference: BE5194). Services for accessing this material are described at the back of the journal.

containing 25% sucrose and 1.7 m*M* SDS and were flash-cooled in liquid nitrogen. Diffraction data were collected on beamline X6A of the National Synchrotron Light Source.

Data were integrated and merged using the program *d*TREK*97 (Pflugrath, 1999). The structures were determined using the difference Fourier technique with PDB entry 1xz1 (Liu *et al.*, 2005) as the starting model. The programs *CNS* (Brunger, 2007), *PHENIX* (Adams *et al.*, 2010), *O* (Jones *et al.*, 1991) and *Coot* (Emsley *et al.*, 2010) were used in refinement and rebuilding. Simulated annealing as implemented in *CNS* was used to remove model bias after initial rigid-body refinement. Water molecules were found using *PHENIX*. Only waters that had peaks in both $F_o - F_c$ and $2F_o - F_c$ maps and were within hydrogen-bonding distance of polar atoms in the protein or other perceived waters were retained for further refinement. Cadmium(II) ions were modeled with the aid of anomalous difference maps. Libraries and idealized coordinates for SDS were obtained from the *PRODRG* server (http://davapc1.bioch.dundee.ac.uk/programs/prodrg; Schüttelkopf & van Aalten, 2004). Ligand occupancy was held fixed at 0.5 during refinement. Data-collection and refinement statistics are shown in Table 1. Coordinates and structure factors for the SDS–apoferritin complex have been deposited in the Protein Data Bank (accession code 3u90).

Ligand and cavity volumes were calculated using the program *VOIDOO* (Kleywegt & Jones, 1994) as described by Vedula *et al.* (2009). As has previously been observed with horse spleen apoferritin (Granier *et al.*, 1997; Liu *et al.*, 2005; Vedula *et al.*, 2009), no evidence of the H chains could be seen in the electron-density map, and thus the protein was modeled as 100% L chain.

2.5. CMC measurements

The critical micelle concentration (CMC) of SDS is strongly dependent upon the ionic strength of the solution (Gunnarsson *et al.*, 1980). Therefore, CMC values were measured in the same buffers as were used for the CD and ITC experiments. CMC measurements were obtained by measuring the enhancement of ANS fluorescence that accompanies micelle formation, as described by Birdi *et al.* (1977). Typical fluorescence titrations can be seen in Fig. S3.

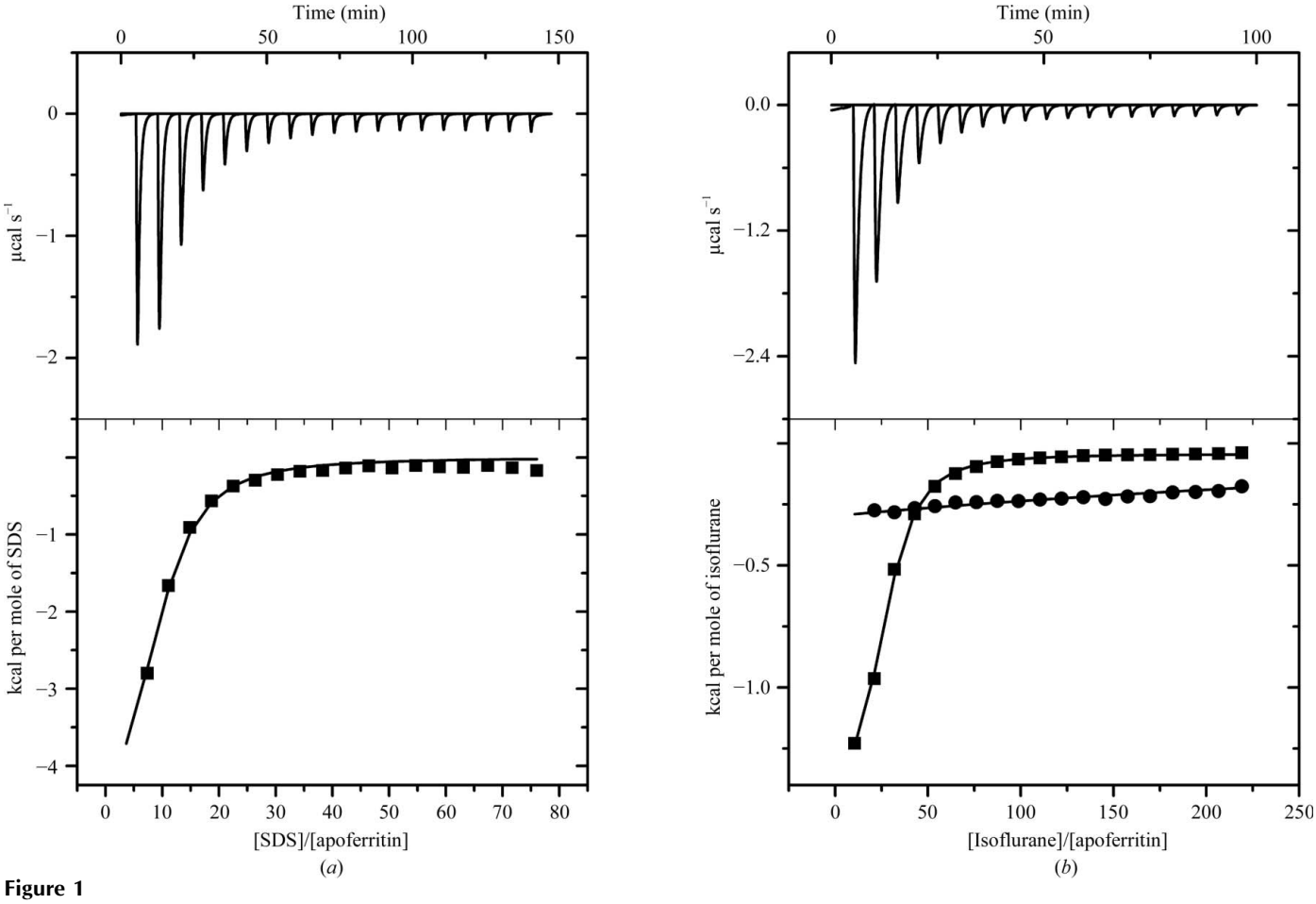

Figure 1
Characterization of the apoferritin–SDS interaction by isothermal titration calorimetry at 293 K. (*a*) Upper panel, enthalpogram corresponding to titration of 3.47 m*M* SDS into 0.01 m*M* apoferritin; lower panel, binding isotherm derived from this titration, indicating a saturable heat-release process. (*b*) Upper panel, enthalpogram corresponding to titration of 10 m*M* isoflurane into 0.01 m*M* apoferritin; lower panel, comparison of binding isotherms for isoflurane with apoferritin in the presence (circles) or absence (squares) of 347 µ*M* SDS. Buffer condition: 130 m*M* NaCl, 20 m*M* sodium phosphate pH 7.0. 1 cal = 4.186 J.

3. Results

3.1. SDS binds to an anesthetic binding site in apoferritin

To test whether binding of SDS to apoferritin could be detected in solution, isothermal titration calorimetry was used. As indicated in Fig. 1(*a*), titration of SDS into apoferritin demonstrated a saturable heat-release process; fitting the data to a single-site model yielded a dissociation constant (K_d) of 24 ± 9 μ*M* at 293 K. ΔH of binding was found to be −21.7 ± 3.8 kJ mol^{-1}, with a $T\Delta S$ value of 4.2 kJ mol^{-1}. The number of sites obtained per apoferritin 24-mer was 8.3 ± 1.1, which is in reasonable agreement with the expected 12 sites (each site lies at a dimer interface between two apoferritin protomers, so there are 12 sites in the apoferritin 24-mer). During the titration, the maximum SDS concentration in the sample cell was 800 μ*M*; the CMC value of the detergent was determined to be 820 ± 56 μ*M* under these conditions (Fig. S3) and so the SDS molecules are expected to behave as monomers throughout the majority of the titration. Pre-saturation of apoferritin with the general anesthetic isoflurane totally abolished the SDS-induced heat release (Fig. S2). Similarly, isoflurane titration into apoferritin also demonstrated saturable binding (Liu *et al.*, 2005) and pre-saturation of apoferritin with SDS inhibited isoflurane binding (Fig. 1*b*). Hence, SDS does bind to apoferritin; furthermore, SDS occupancy competes with the binding of general anesthetics. This competition between SDS and isoflurane suggests that SDS binds to the anesthetic site in apoferritin where isoflurane, halothane, propofol and thiopental have previously been shown to bind by X-ray crystallography (Liu *et al.*, 2005; Vedula *et al.*, 2009).

3.2. SDS at low concentration does not perturb apoferritin secondary structure

Because SDS is a well known protein denaturant, we used circular dichroism to test whether the detergent was exerting any denaturing effect on apoferritin at the micromolar concentrations required for binding. The CD spectrum of 1 μ*M* apoferritin was measured in the presence of 347 μ*M* SDS (Fig. 2). Based on the K_d of 24 μ*M* determined from our ITC experiments, the apoferritin site should be greater than 90% occupied at these concentrations. Under these conditions, the far-UV CD spectrum of apoferritin was found to be identical to that of the detergent-free protein, indicating that the binding of SDS to apoferritin does not grossly alter the protein structure. The SDS concentration in the CD experiment is well below the CMC value of the detergent under these conditions, which was found to be 3.55 ± 0.04 m*M* (Fig. S3).

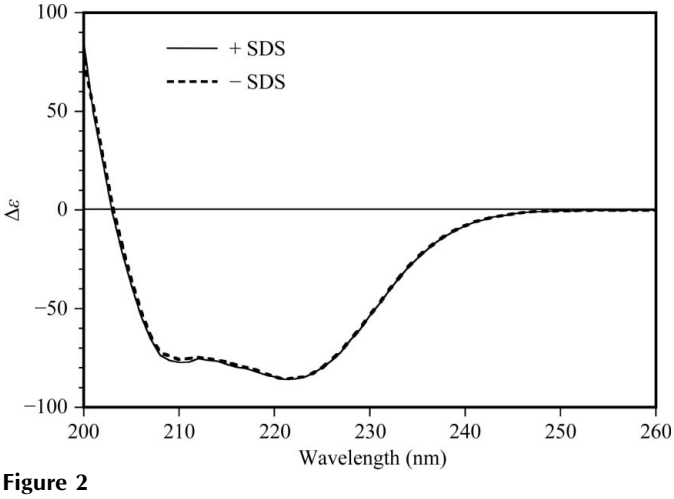

Figure 2
CD spectra of 1 μ*M* apoferritin in the presence (solid line) and absence (dashed line) of 347 μ*M* SDS. No significant spectral change is observed.

3.3. Crystal structure of the SDS–apoferritin complex

In order to determine the structural details of how apoferritin recognizes SDS, the protein was cocrystallized with the detergent. Initial difference maps calculated after rigid-body refinement clearly showed the presence of a U-shaped electron density which was not observed with data collected from crystals containing no SDS. Consistent with the solution binding data, this difference density is seen in the same cavity that forms the binding site for isoflurane and other anesthetics. SDS was easily modeled into the difference density and refined well (Fig. 3).

The ligand-binding cavity in apoferritin lies at the interface between two protomers; it is largely buried, but is connected to the exterior of the protein by two small openings. The polar head group of the SDS molecule is situated in the opening of the cavity, interacting with polar side chains on the protein-cavity surface (Fig. 4). The dodecyl chain of the detergent penetrates into the hydrophobic cavity, bending into a

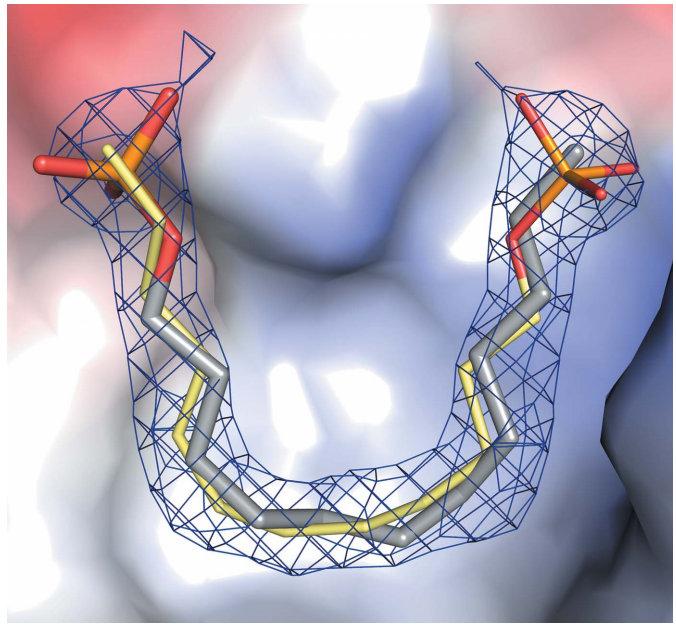

Figure 3
OMIT $2F_o - F_c$ electron density for the SDS ligand contoured at 1.0σ. The two symmetry-related conformations of the SDS molecule are shown; the C atoms of one conformer are colored gray and those of the other yellow. S atoms are shown in orange and O atoms in red. In the background an electrostatic surface calculated for the apoferritin protein can be seen.

horseshoe shape to conform to the shape of the binding cavity. The cavity lies directly on a crystallographic twofold axis of symmetry that relates two apoferritin protomers, both of which contribute residues that form the ligand-binding cavity. Owing to the twofold-symmetric nature of the binding cavity, the SDS ligand can adopt one of two possible conformations in any given cavity. These two conformations are related to one another by a 180° rotation and are mutually exclusive owing to almost complete overlap. Therefore, the maximum occupancy of each SDS conformer is 0.5 and the observed electron density corresponds to the average of the two conformers.

The two symmetry-related copies of Arg59 form the lid of the ligand-binding cavity. Two symmetric apertures on either side of these two side chains lead into the cavity. The sulfate head group of the SDS molecule sits in the cavity opening, close to both Arg59 side chains (the distance of closest approach is 3.3 Å for one copy of the arginine side chain and 4.1 Å for the other; see Fig. 4). The side-chain hydroxyl of Ser27 lies 3.4 Å away from the SDS ester O atom and thus may be able to contribute a hydrogen bond to the ligand. The side chain of Glu63, which forms a salt bridge with the Arg59 side chain (oxygen–nitrogen distance of 2.7 Å), is also close to the sulfate head group of the SDS molecule (oxygen–oxygen distance of 2.5 Å); presumably, any electrostatic repulsion between the glutamate and the SDS is countered by the favorable interactions between the SDS head group and the two arginines. The Glu63 side chain is also close to the Arg52 side chain (2.9 Å), which contributes additional positive charge that should further counter any charge repulsion between the glutamate and the SDS ligand. Ions in the solvent are also likely to associate with these charged groups, but no well ordered ions were observed bound to the sulfate head group in the crystal structure. The hydrophobic detergent tail is buried within the cavity, which is largely lined by hydrophobic residues. However, the dodecyl tail makes few close contacts within the cavity. The only protein residues that approach to within van der Waals distance of the SDS tail are Ser27, Ala55 and Arg59.

As has been reported previously (Granier *et al.*, 1997), no evidence for the apoferritin heavy chain can be seen in the electron-density map, consistent with the low level (∼10%) of H chain estimated to be present. However, alignment of the H-chain and L-chain structures reveals that the residues that are close to the SDS ligand are either completely conserved in the H chain (Leu24, Ser27, Tyr28, Leu31, Arg59 and Glu59) or only slightly different (the residue corresponding to Ala55 in the heavy chain is a serine). Thus, one can speculate that the SDS ligand should be able to bind to binding sites composed of one heavy and one light chain (H:L), as well as L:L binding sites (H:H sites, while theoretically possible, should be very rare if heavy chains are incorporated randomly into the 24-mer).

The presence of the SDS ligand does not cause any perturbation in the apoferritin backbone conformation; superposition of the apoferritin–SDS complex structure with the apoferritin–propofol or apoferritin–isoflurane complex structures (PDB entries 3f33 and 1xz3, respectively; Vedula *et al.*, 2009; Liu *et al.*, 2005) or with unliganded apoferritin (PDB entry 3f32; Vedula *et al.*, 2009) results in all cases in r.m.s. differences in C^{α} positions of less than 0.2 Å. Inspection of the superposed structures reveals no obvious local differences in backbone structure and only minor differences in side-chain positions.

4. Discussion

SDS has long been synonymous with protein denaturation and nonspecific interactions and it is therefore interesting that at modest SDS concentrations apoferritin recognizes SDS specifically, with the ligand occupying a well defined binding site in an internal protein cavity. The specific nature of this binding is borne out by the saturable nature of the ITC isotherm, the lack of alteration of the protein secondary structure (as detected by circular dichroism) and the protein tertiary structure (as detected by X-ray crystallography) and the unambiguous electron density seen for the ligand in the crystal structure.

This X-ray structure is not the first to demonstrate SDS binding to a protein. We found three other SDS-containing crystal structures in the Protein Data Bank: cardiotoxin A3 (PDB entry 1h0j; Forouhar *et al.*, 2003), chicken lysozyme (PDB entry 3b6l; Michaux *et al.*, 2008) and PagP (PDB entry 3gp6; Cuesta-Seijo *et al.*, 2010). Cardiotoxin A3 is a membrane-

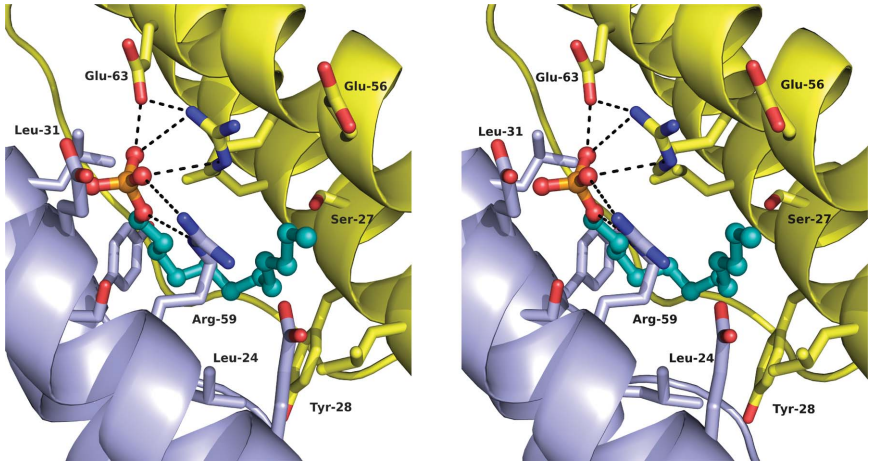

Figure 4
Stereoview of the SDS binding pocket. The pocket lies at the interface between two protomers in the ferritin 24-mer; one protomer is shown in yellow and the other in blue. The two protomers are related by a twofold crystallographic axis of symmetry that passes through the center of the binding pocket and thus each side chain that contributes to forming the pocket is present as two copies (only one copy of each side chain is labeled in the figure for the sake of clarity). The SDS molecule is shown in a ball-and-stick representation with the following color scheme: oxygen, red; sulfur, orange; carbon, teal. Polar interactions between the SDS sulfate head group and the side chains of Arg59 and Glu63 are shown as dashed lines.

active molecule and its structure in the presence of SDS reveals three detergent molecules arrayed along one face of the molecule, apparently identifying the face that interacts with the membrane (Forouhar *et al.*, 2003). The lysozyme structure was obtained using protein that was refolded from an SDS solution; it shows a single SDS molecule binding to the protein surface (Michaux *et al.*, 2008). It is noteworthy that the lysozyme crystals were grown in the presence of high concentrations of the amphiphilic molecule 2-methyl-2,4-pentanediol (MPD), which appears to counter the denaturing effects of the SDS. In the absence of MPD, SDS molecules denature lysozyme by binding to an internal site located between two lobes of the protein, pushing them apart (Yonath *et al.*, 1977). The PagP structure also corresponds to a protein refolded from a solution containing both SDS and MPD. PagP is an integral membrane protein and not surprisingly the structure shows five SDS molecules adsorbed onto the hydrophobic surface of the protein, more than the number that bind to the surfaces of the soluble proteins lysozyme or cardiotoxin A3 (Cuesta-Seijo *et al.*, 2010). In addition, a sixth SDS molecule is bound in an internal PagP site. PagP is a bacterial fatty-acid transferase that recognizes a palmitate-containing substrate, and the alkyl chain of the SDS molecule in this internal site occupies the recognition pocket for the fatty-acyl group.

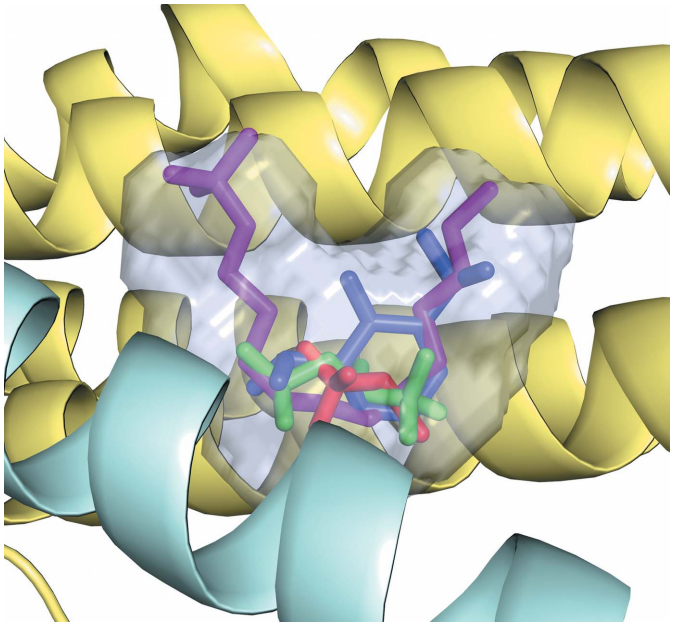

Figure 5
SDS shares a common binding site with general anesthetics. A superposition of four different ligands in the common apoferritin binding pocket is shown. Color scheme: SDS, purple; propofol, blue; halothane, red; isoflurane, green. The cavity volume as calculated using *VOIDOO* is shown as a transparent surface.

Apoferritin differs from these examples in two important ways. Firstly, the SDS concentration used in its crystallographic analysis is considerably lower than those used for the other proteins, reflecting the relatively high affinity of SDS for the apoferritin ligand-binding site. Secondly, no ordered SDS molecules are seen to be adsorbed onto the apoferritin outer or inner protein surfaces; instead, only a single SDS molecule binds in an internal cavity, the same site that has been shown to bind many general anesthetics, including both inhaled and intravenous agents (Fig. 5; Butts *et al.*, 2009; Liu *et al.*, 2005; Vedula *et al.*, 2009). This site has also been reported to bind other amphipathic molecules (Niemeyer *et al.*, 2008; Trikha *et al.*, 1995). In the evolutionarily related bacterioferritins the corresponding site serves to bind heme (Carrondo, 2003), and horse spleen apoferritin retains the ability to bind porphyrin in this site (Précigoux *et al.*, 1994). In the horse ferritin–porphyrin complex structure the hydrophobic ring structure binds in the heart of the cavity, while the propionic acid side chains extend out from the openings to this cavity, where they can interact with the two symmetry-related copies of Arg59 in a manner similar to that seen with SDS.

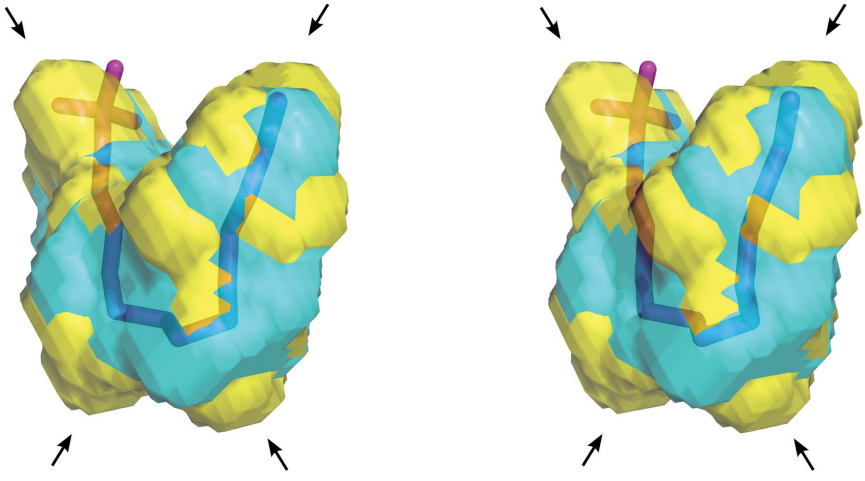

Figure 6
Stereo image comparing apoferritin cavity volumes in the SDS-bound complex (yellow) and in the ligand-free protein (cyan). While the overall sizes and shapes of the two cavities are similar, in the presence of SDS the cavity size increases significantly. The increase in volume is not isotropic, but is rather concentrated in several lobes at the top and bottom of the cavity (indicated by arrows).

The nature of SDS recognition within the apoferritin cavity is consistent with the amphipathic character of the ligand. The charged sulfate head group is located at the protein inner surface, where it interacts with charged protein side chains and is also accessible to solvent molecules. The hydrophobic tail inserts into the apolar cavity, where it is shielded from solvent. The alkyl tail is ordered in the crystal structure, displaying good electron density and reasonable atomic displacement parameters. Despite its degree of order, however, it does not make intimate interactions with residues that line the cavity, even though most of them are nonpolar or amphipathic. A similar kind of packing is seen for the SDS molecule that binds in the fatty-acyl pocket

of PagP (Cuesta-Seijo *et al.*, 2010); its tail is well ordered and surrounded by hydrophobic residues but makes close approaches to only a few of these residues. This is likely to reflect an enthalpy–entropy tradeoff: because there are no strong interactions between the detergent tail and the protein, enthalpic contributions to affinity are limited to relatively weak van der Waals forces. Immobilizing the ligand too tightly will exact a high entropic cost that cannot be compensated by this small enthalpic contribution and so hydrophobic ligands are predicted to be held relatively loosely within such cavities, corresponding to packing densities of the order of 0.55 (Mecozzi & Rebek, 1998). When polar interactions are present, however, this situation does not necessarily pertain because polar interactions can contribute relatively large enthalpies of binding that compensate for the entropy losses associated with tighter immobilization (and correspondingly higher packing densities). For the apoferritin–SDS complex the calculated cavity volume is 420 ± 11 Å^3, while the ligand volume is 260 ± 0.4 Å^3, corresponding to a packing density of 0.62 ± 0.02. SDS is the largest apoferritin ligand for which a crystal structure is available to date and the cavity volume is one of the largest seen for an apoferritin–ligand complex. Interestingly, the expansion of the cavity involves neither major backbone movements by the protein nor changes in intersubunit distances; instead, the increase in volume is achieved by subtle movements of amino-acid side chains, which cause the cavity to bulge outward at several spots (Fig. 6). The packing density for SDS is considerably higher than the values observed for more hydrophobic ligands such as anesthetics (Vedula *et al.*, 2009), so a favorable enthalpic component to binding contributed by the charged detergent head group may help to compensate for the entropically unfavorable immobilization of this relatively large ligand in the apoferritin cavity. Consistent with this picture, SDS binding to apoferritin is characterized by a modest but favorable ΔH ($\simeq -21$ kJ mol^{-1}) and an almost negligible entropic component ($T\Delta S \simeq -4$ kJ mol^{-1}). Caution should be employed in interpreting these data, however, as hydrophobic effects can manifest enthalpically as well as entropically (Snyder *et al.*, 2011).

In addition to its use in basic science research, SDS is ubiquitous in medical applications. Among other things, it is a component of toothpaste, it is used as a laxative in enemas, it serves as an excipient in aspirin and fiber-therapy caplets and it has been investigated as a microbiocide (Piret *et al.*, 2000, 2002). Most of these applications are assumed to rely upon the surfactant properties of the molecule. However, evidence is now emerging that SDS can also generate particular pharmacological effects distinct from its detergent actions through specific binding to protein targets. This means that SDS might provide useful information about ligand-binding sites for particular protein targets. For example, SDS modulates the activity of the neutrophil formyl-peptide receptor (Thorén *et al.*, 2010); this G-protein-coupled receptor is an important therapeutic target for anti-inflammatory agents and selective antagonists have potential utility in the treatment of many pathological processes, including rheumatoid arthritis, sepsis, septic shock, asthma and Alzheimer's disease (Forsman *et al.*, 2011). SDS might provide a useful new lead compound in the effort to develop such agents.

In conclusion, we provide structural and biophysical evidence that SDS can specifically bind to a naturally occurring mammalian protein, apoferritin. The structural details of how ferritin recognizes SDS may prove useful in developing SDS-like molecules for potential clinical applications.

The authors acknowledge excellent technical support from Dr Min Li and valuable discussions with Drs Roderic G. Eckenhoff and Renlong Zhou. This work was partially funded by NIH grants K08-GM093115 (RL) and P01-GM55876 (PJL) and NSF CAREER award CHE 0548188 (IJD). Support was also provided by the Department of Anesthesiology and Critical Care at the University of Pennsylvania.

References

Adams, P. D. *et al.* (2010). *Acta Cryst.* D**66**, 213–221.
Birdi, K. S., Krag, T. & Klausen, J. (1977). *J. Colloid Interface Sci.* **62**, 562–563.
Brunger, A. T. (2007). *Nature Protoc.* **2**, 2728–2733.
Butts, C. A., Xi, J., Brannigan, G., Saad, A. A., Venkatachalan, S. P., Pearce, R. A., Klein, M. L., Eckenhoff, R. G. & Dmochowski, I. J. (2009). *Proc. Natl Acad. Sci. USA*, **106**, 6501–6506.
Carrondo, M. A. (2003). *EMBO J.* **22**, 1959–1968.
Clark, R. A., Leidal, K. G., Pearson, D. W. & Nauseef, W. M. (1987). *J. Biol. Chem.* **262**, 4065–4074.
Crichton, R. R. & Declercq, J. P. (2010). *Biochim. Biophys. Acta*, **1800**, 706–718.
Cuesta-Seijo, J. A., Neale, C., Khan, M. A., Moktar, J., Tran, C. D., Bishop, R. E., Pomès, R. & Privé, G. G. (2010). *Structure*, **18**, 1210–1219.
Emsley, P., Lohkamp, B., Scott, W. G. & Cowtan, K. (2010). *Acta Cryst.* D**66**, 486–501.
Forouhar, F., Huang, W.-N., Liu, J.-H., Chien, K.-Y., Wu, W. & Hsiao, C.-D. (2003). *J. Biol. Chem.* **278**, 21980–21988.
Forsman, H., Kalderén, C., Nordin, A., Nordling, E., Jensen, A. J. & Dahlgren, C. (2011). *Biochem. Pharmacol.* **81**, 402–411.
Granier, T., Gallois, B., Dautant, A., Langlois d'Estaintot, B. & Précigoux, G. (1997). *Acta Cryst.* D**53**, 580–587.
Gunnarsson, G., Jonsson, B. & Wennerstrom, H. (1980). *J. Phys. Chem.* **84**, 3114–3121.
Harrison, P. M. & Arosio, P. (1996). *Biochim. Biophys. Acta*, **1275**, 161–203.
Jones, T. A., Zou, J.-Y., Cowan, S. W. & Kjeldgaard, M. (1991). *Acta Cryst.* A**47**, 110–119.
Kleywegt, G. J. & Jones, T. A. (1994). *Acta Cryst.* D**50**, 178–185.
Liu, R. & Eckenhoff, R. G. (2005). *Anesthesiology*, **102**, 799–805.
Liu, R., Loll, P. J. & Eckenhoff, R. G. (2005). *FASEB J.* **19**, 567–576.
Mecozzi, S. & Rebek, J. J. (1998). *Chem. Eur. J.* **4**, 1016–1022.
Michaux, C., Pouyez, J., Wouters, J. & Privé, G. G. (2008). *BMC Struct. Biol.* **8**, 29.
Niemeyer, J., Abe, S., Hikage, T., Ueno, T., Erker, G. & Watanabe, Y. (2008). *Chem. Commun.*, pp. 6519–6521.
Pflugrath, J. W. (1999). *Acta Cryst.* D**55**, 1718–1725.
Piret, J., Désormeaux, A. & Bergeron, M. G. (2002). *Curr. Drug Targets*, **3**, 17–30.
Piret, J., Lamontagne, J., Bestman-Smith, J., Roy, S., Gourde, P., Désormeaux, A., Omar, R. F., Juhász, J. & Bergeron, M. G. (2000). *J. Clin. Microbiol.* **38**, 110–119.
Précigoux, G., Yariv, J., Gallois, B., Dautant, A., Courseille, C. & Langlois d'Estaintot, B. L. (1994). *Acta Cryst.* D**50**, 739–743.

Schüttelkopf, A. W. & van Aalten, D. M. F. (2004). *Acta Cryst.* D**60**, 1355–1363.
Snyder, P. W., Mecinovic, J., Moustakas, D. T., Thomas, S. W. III, Harder, M., Mack, E. T., Lockett, M. R., Heroux, A., Sherman, W. & Whitesides, G. M. (2011). *Proc. Natl. Acad. Sci. USA*, **108**, 17889–17894
Thorén, F. B., Karlsson, J., Dahlgren, C. & Forsman, H. (2010). *Biochem. Pharmacol.* **80**, 389–395.
Trikha, J., Theil, E. C. & Allewell, N. M. (1995). *J. Mol. Biol.* **248**, 949–967.
Vedula, L. S., Brannigan, G., Economou, N. J., Xi, J., Hall, M. A., Liu, R., Rossi, M. J., Dailey, W. P., Grasty, K. C., Klein, M. L., Eckenhoff, R. G. & Loll, P. J. (2009). *J. Biol. Chem.* **284**, 24176–24184.
Yang, L. & Sonner, J. M. (2008). *Anesth. Analg.* **106**, 838–845.
Yonath, A., Podjarny, A., Honig, B., Sielecki, A. & Traub, W. (1977). *Biochemistry*, **16**, 1418–1424.